Photocurrent enhancement in silicon photodiodes with Ge quantum dots by hybrid plasmonic and dielectric modes of a planar waveguide

© A.I. Yakimov[1], V.V. Kirienko[1], A.A. Bloshkin[1,2], A.V. Dvurechenskii[1,2], D.E. Utkin[1,2]

[1] Rzhanov Institute of Semiconductor Physics, Siberian Branch, Russian Academy of Sciences,
630090 Novosibirsk, Russia
[2] Novosibirsk State University,
630090 Novosibirsk, Russia

E-mail: andrewyakimov5@gmail.com

Received August 2, 2024
Revised August 27, 2024
Accepted September 3, 2024

The spectral characteristics of the near-infrared photocurrent in vertical Ge/Si photodiodes with Ge quantum dots embedded in a planar waveguide and coupled with a plasmonic structure on the surface of the photodiode are studied. A two-dimensional regular lattice of circular holes in an aluminum film acted as a plasma metasurface, allowing the conversion of external electromagnetic radiation into surface plasmon modes at the Al-Si boundary. The diameter of the holes is 300 nm, the period is 600 nm. In the wavelength range of $\sim 2\mu$, a series of optical resonances was detected, leading to a multiple amplification of the photocurrent compared with samples without perforated Al film. It is established that the maximum amplification of the photocurrent (up to 8 times) is provided by hybrid waves, which are a superposition of plasmonic and dielectric waveguide modes.

Keywords: optical telecommunication, quantum dots Ge/Si, surface plasmonic waves, waveguide modes.

DOI: 10.61011/SC.2024.07.59545.6952

1. Introduction

Enlargement of the spectral range of the silicon-based optical elements up to the wavelength of $\sim 8\,\mu$m becomes possible due to the use of the flawless Ge/Si heterostructures with Ge quantum dots (QD) capable of registering the optical emission both in the near, and in the middle infrared (IR) bands [1,2]. Being easily integrated into various metamaterials, Ge QDs allow designing a new generation of integrated silicon photonics devices, where the operating wavelength range is controlled by the size and design of the metamaterial. The problem limiting the widespread use of Ge/Si QDs is the low coefficient of light absorption by quantum dots. In this regard, a series of fundamental problems arises related to the search for physical mechanisms that provide a significant increase in optical absorption and photocurrent in heterostructures with QD.

The simplest and most common approach to achieve higher absorption of optical radiation in thin low-absorbing semiconductor layers is the use of waveguide structures [3–5]. Thus, for instance, if the layers with quantum dots may be placed on the silicon-on-insulator substrate (SOI), then because of the difference in the refractive indices Si and SiO_2 the light wave field will be clamped between the buried oxide layer and surface of heterostructure with minimal intensity in the quantum dots domain. Enhancement of photocurrent in SOI structures is the result of Fabry-Perot vertical resonances caused by the interface of waves reflected from the air/Si and Si/SiO_2 interfaces. However, the enhancement factor is small and rarely exceeds 100% due to large losses at the boundaries.

It is possible to increase the absorption coefficient in a thin semiconductor layer by integrating dielectric waveguides with various types of metastructures, in particular with metallic plasmonic metasurfaces [6–11]. In the last decade, plasmonics has become a powerful branch of science, which has allowed to obtain breakthrough results in the field of biosensorics and molecular spectroscopy, create the ultra-dense memory elements, increase the efficiency of optoelectronic devices such as solar cells, radiation sources, semiconductor lasers and photodetectors [12–15]. For the perforated thin metal films with sub-wavelength periodic holes on the surface of heterostructures with Ge/Si and InGaAs quantum dots there was found a multiple (up to 40 times) increase of photocurrent within middle IR spectral range of $3-5\,\mu$m [20–22] and $8-14\,\mu$m [23–25]. Further theoretical analysis showed [26] that plasmon effects should also be expected in the near-IR region of the spectrum, since in this wavelength range the real part of the dielectric function of most metals is negative. However, until recently, it was not possible to create real plasmon structures integrated with perforated metal films for the near-infrared range (in the field of optical telecommunications), since this requires holes with a period of location and a diameter of a nanometer scale.

In this study the optical resonances in the near IF domain in the hybrid Ge/Si *pin*-photodiodes (PD) with Ge quantum dots grown on SOI substrates and conjugated with the plasmon grating of nano-holes in AL film on the heterostructure surface. The holes diameter was 300 nm, grating period — 600 nm. Two types of planar waveguide modes excited by light radiation at different wavelengths have been discovered. The first type corresponds to

plasmon-polariton waves propagating along the boundary of Al-Si. The second type is hybrid in nature and is a superposition of plasmonic and dielectric waveguide modes. It is the hybrid modes that ensure the maximum increase in the absorption of optical radiation in QD layers.

2. Experiment procedure

They were grown by method of the molecular-beam epitaxy on SOI substrates and represented themselves vertical *pin*-photodiodes with a diameter of 700 μm (Figure 1, *a*). A detailed description of the electronic structure of Ge/Si QDs and growth conditions, such as temperature and deposition rate of materials, was presented earlier in paper jcite27. For the synthesis of Ge QDs arrays, the phenomenon of self-organization of semiconductor nanostructures during materials heteroepitaxial growth with a large grating parameters mismatch was used. Density, sizes and QD elements are described in paper [28].

Next, a metallic plasmonic structure was fabricated on the PD surface by applying Al film with a thickness of 50 nm and forming a square lattice of round holes in it using electronic lithography (Figure 1, *b*). Holes diameter $d = 300$ nm, grating period $p = 600$ nm. The surface portion occupied by holes in Al, was 19.6%. To identify the optical resonances related to the plasmon effects similar *pin*-PD Ge/Si with Ge QD on SOI were fabricated. Their difference from plasmon photodetectors was only in the absence of a perforated aluminum film on the surface. To determine the effect of Ge quantum dots on the photocurrent spectra, a reference Si photodiode without Ge and nanostructured Al film was fabricated in conditions similar to those described above.

The photoresponse was measured at room temperature using Fourier transform spectrometer Bruker Vertex-70 with a resolution of 10 cm^{-1}. The photodiodes were exposed from the side of the plasmon grating normal to the samples surface along z. The light was linearly polarized, and the electric field vector in the incident electromagnetic wave was directed along the axis x in the plane of the heterostructure.

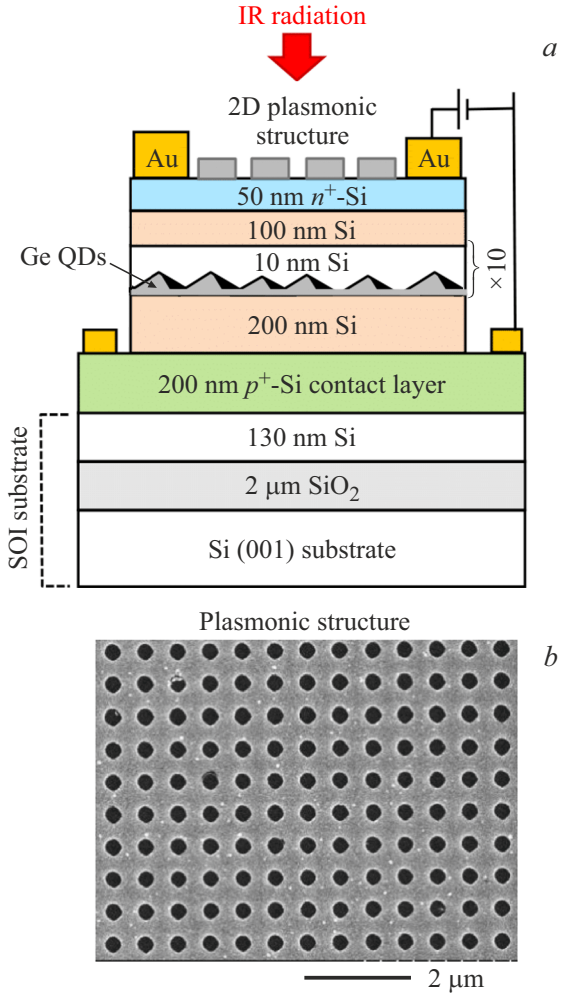

Figure 1. Section of vertical *pin*-photodiode with Ge quantum dots in Si matrix on SOI substrate mated with a 2D sub-wavelength holes plasmon grating in Al film (*a*). Image of perforated Al film on the photodiode surface obtained by scanning electron microscopy (*b*). Holes diameter — 300 nm, grating period — 600 nm.

3. Results and discussion

Figure 2 illustrates the spectral characteristics of the current sensitivity of three samples grown on SOI substrate. The first sample doesn't contain neither Ge QDs, nor the surface plasmon structure (curve *1*). The second sample is a Ge/Si photodiode with Ge quantum dots, but without perforated Al film (curve *2*). The third detector differs from the second one by presence of the 2D plasmon metastructure on the detector surface (curve *3*). Wide photocurrent resonances are observed in the spectra of all three samples caused by interference of waves reflected from the air/Si and Si/SiO_2 interfaces. Their spectral position on the wavelength scale is determined by the thickness of the silicon layer located between the air and the buried SiO_2. This thickness is the same for the test photodiode, reference diode without plasmon Al film, but containing 10 layers of Ge quantum dots (curve *2*), and hybrid Ge/Si photodiode with Ge quantum dots, with the perforated Al film located on the photodiode surface (curve *3*). Therefore, the locations of these resonances are close for all samples. The long-wavelength edge of the reference photodiode makes $\sim 1.3\,\mu$m. The response of the photodiode with Ge QDs covers a wider spectral range up to 1.9 μm and is caused by inter-band transitions between the electronic states in the conduction band and hole states inside Ge quantum dots.

The implementation of a plasmon grating on the surface of Ge/Si photodiode makes it possible to increase the detector sensitivity in many times and shift its long-wavelength boundary to 2.1 μm. The highest growth of the photocurrent is observed in the long-wavelength spectrum

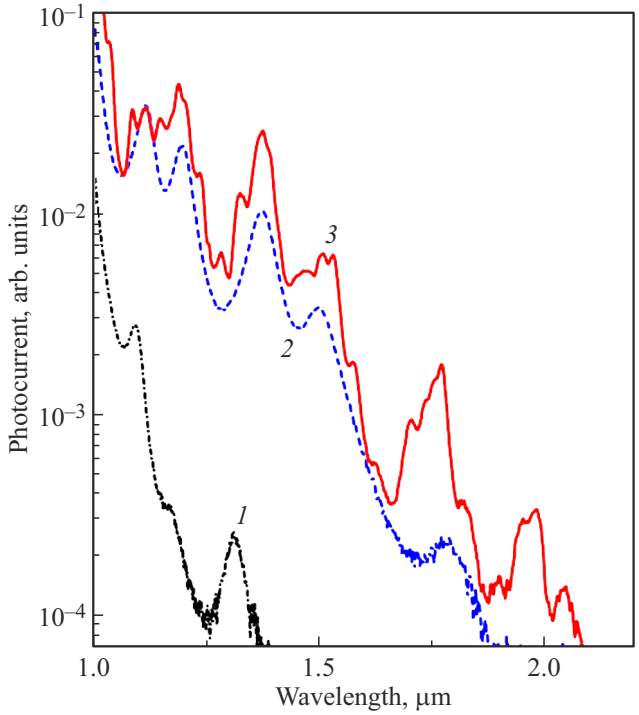

Figure 2. Photocurrent spectra of the test*pin*-photodiode without Ge QDs and without surface plasmon structure (*1*), reference diode without plasmon Al film, but containing 10 layers of Ge QDs(*2*), and hybrid Ge/Si photodiode with Ge QDs,on the surface of which the perforated Al film is placed (*3*). The measurements were performed at room temperature at a reverse bias voltage of 2 V.

area — in the area of wavelengths of $1.7-2.1\,\mu$m. This circumstance seems to be extremely important, since it is in this communication window where function the new generation hollow-core fiber optics and fiber-optic amplifiers doped with thulium [29–31]. To define the additional resonances, associated with the plasmon grating, in presence of Fabry-Perot resonances, the photocurrent enhancement factor K, is generally analyzed; this enhancement factor is defined as a ratio of spectral characteristics of PD photocurrent with the plasmonic structure and without it (Figure 3). It is this technique that makes it possible to identify the contribution of the plasmonic structure to the spectral composition of the photocurrent.

The law of dispersion of surface plasmons at the metal-dielectric interface is given by the expression [32]

$$k_{SP} = \frac{\omega_{SP}}{c}\sqrt{\frac{\epsilon_m\epsilon_d}{\epsilon_m+\epsilon_d}}, \qquad (1)$$

where k_{SP} — wave vector of the surface plasmon wave, ω_{SP} — its frequency, c — light speed in vacuum, ϵ_m and ϵ_d — dielectric functions of metal and dielectric. The speed of the surface plasmon wave in this case is defined as

$$s = c\sqrt{\frac{\epsilon_m+\epsilon_d}{\epsilon_m\epsilon_d}} \approx \frac{c}{\sqrt{\epsilon_d}}. \qquad (2)$$

In the light wavelength range of $\sim 2\,\mu$m, which were used in the experiment, the dielectric function of silicon is ~ 12. The dielectric function of aluminum varies from $-88.100 + i \cdot 27.27$ at the wavelength of $1\,\mu$m to $-623.29 + i \cdot 170.38$ at the wavelength of $2.5\,\mu$m [33]. Throughout this band, the dielectric function of the metal is much higher than the dielectric function of the dielectric, therefore, in the first approximation, the velocity of the surface plasmon wave can be considered 3.5 times less than the speed of light. To excite the plasmon by electromagnetic wave field the ratios $k_{\|} = k_{SP}$ and $\omega = \omega_{SP}$ shall be fulfilled, where $k_{\|}$, ω — component of the light wave vector parallel to the metal-dielectric interface, and frequency of the incident electromagnetic wave. According to equation (1), both these conditions cannot be fulfilled in case of a flat metal/dielectric interface. For excitation of the surface plasmon waves various methods are used, e.g., diffraction grating method, when the wave vector of the incident electromagnetic wave is transformed into a set of vectors $k_{\|} \to k_{\|} \pm G$, where $G = \frac{2\pi m}{p}e_x + \frac{2\pi n}{p}e_y$, m, n — arbitrary integer numbers, p — period of surface diffraction grating, and e_x and e_y — unit vectors oriented along the main axes of the square grating. For normal light incidence $k_{\|} = 0$ and

$$|k_{SP}| = |G|. \qquad (3)$$

By combining (1) and (3), we obtain the following expression for the light wave lengths when plasmon resonances may occur:

$$\lambda_{mn} = \frac{p}{\sqrt{m^2+n^2}}\sqrt{\frac{\epsilon_m\epsilon_d}{\epsilon_m+\epsilon_d}}. \qquad (4)$$

Having taken the frequency dependent dielectric functions ϵ_d, ϵ_m from paper [33], for the grating period $p = 600$ nm, we obtain that every expected wavelength is equal $\lambda_{01} = 2.05\,\mu$m for the fundamental plasmonic mode and $\lambda_{11} = 1.44\,\mu$m for the next order plasmonic mode.

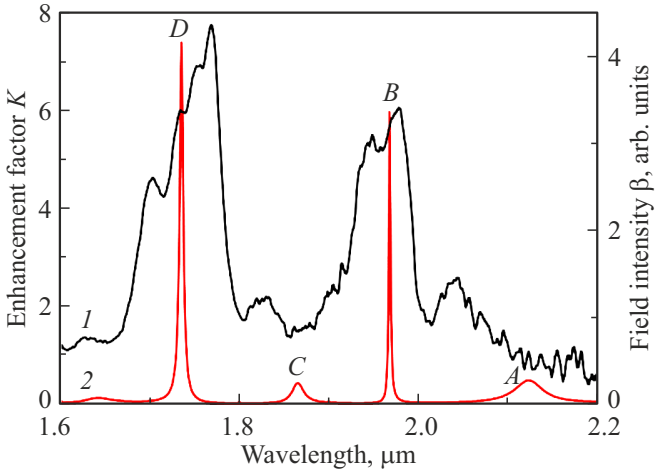

Figure 3. Spectral characteristics of experimental photocurrent enhancement factor (*1*) and rated integral intensity of near field in QD layers (*2*) conjugated with plasmon grating.

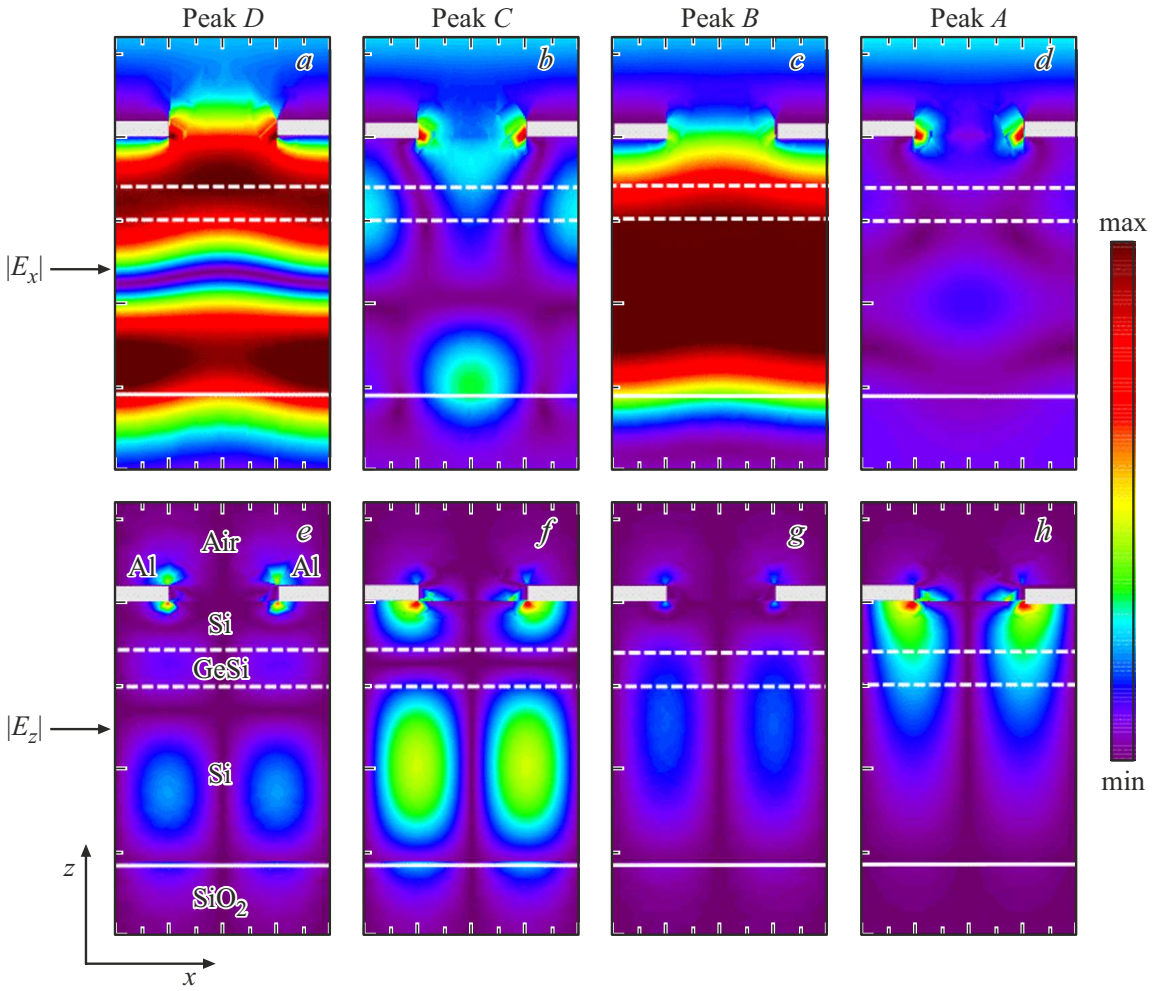

Figure 4. The spatial distribution of electrical field components $|Ex|$ $(a-d)$ and $|Ez|$ $(e-h)$ in $x-z$ plane passing through the center of hole in Al film, at different wavelengths, corresponding to resonances *A, B, C* and *D* in Figure 3. The color scale is the same for all panels. The light is linearly polarized along x axis and falls along the normal to the surface of the structure. The cross-section of the perforated Al film is shown as grey rectangles. The dotted lines indicate the area occupied by Ge QDs. (A color version of the figure is provided in the online version of the paper).

Figure 3 shows the factor of the photocurrent enhancement by plasmon grating K within the wavelengths $1.6-2.2\,\mu$m (curve *1*). Two intensive resonances are observed at the wavelengths of 1.77 and $1.98\,\mu$m with eightfold and sixfold increase of the photocurrent relative to the photodiode without plasmonic structure, respectively. Apart from these lines, the weaker maxima are registered at the wavelengths of 1.83 and $2.05\,\mu$m with $K \simeq 2.2-2.6$. It should be noted that the wavelength of $2.05\,\mu$m coincides with λ_{01} for the plasmon polariton resonance.

In order to clarify the nature of electromagnetic excitations leading to a resonant enhancement of photocurrent, we studied the electric fields that arise when a plasmon detector is irradiated with light. Modeling of the three-dimensional distribution of the electromagnetic field was carried out in the Comsol Multiphysics software by the finite element method. In details this method of calculations is described, e. g., in paper [26]. The spectral characteristic of the integral intensity of the near field $\beta(\lambda)$ for linear polarization of light is given in Figure 3 (curve *2*). Integration takes place in the volume where the layers with quantum dots are located. In area $1.7-2.1\,\mu$m on $\beta(\lambda)$ curve four resonances are observed denoted by letters *A, B, C, D*. In general, the consistency of the calculated position of the near-field peaks and the experimental position of the photocurrent enhancement maxima, as well as their relative intensity, can be considered good. The experimental resonances of the photocurrent are much wider than the theoretical peaks of the near-field intensity. Apparently, this is due to the heterogeneous distribution of the sizes and shapes of the holes, as well as the period of their location in the real grating.

The spatial distributions of the vertical $|E_z|$ components of the electric field and the components $|E_x|$ parallel to the plane of the structure are shown in Figure 4. The images are plotted in section $x-z$, passing through the center of hole in Al film. The selected wavelengths correspond to the

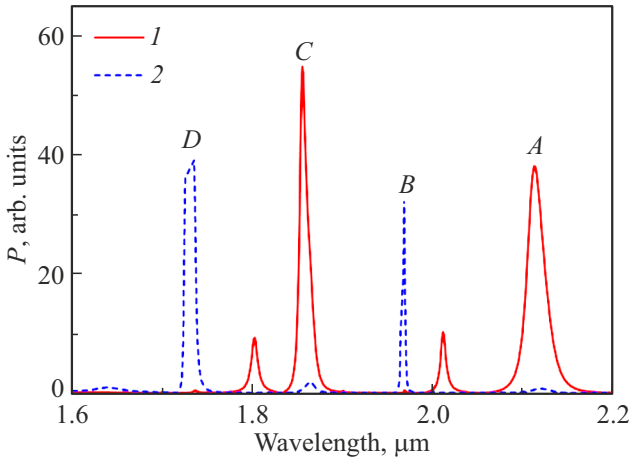

Figure 5. The spectral characteristics are provided for the power of electromagnetic wave, passing through the boundary of the unit cell in directions x (*1*) or y (*2*), calculated by formula (5).

resonances *A, B, C* and *D*. A detailed analysis showed that for all four resonances the electric field component $|E_y| = 0$.

Figure 5 shows the predominant direction of propagation of various modes. Here, the spectral characteristics are provided for the power of electromagnetic wave, passing through the boundary of the unit cell in directions x (curve *1*) or y (curve *2*). Power P was calculated as

$$P = \int_A \vec{S} d\vec{A}, \qquad (5)$$

where $\vec{S}$ — Poynting vector for electromagnetic wave, A — area of the side facet of the unit cell in the analyzed area. The integration was carried out over the area occupied by the silicon layer between the SiO_2 layer and the perforated aluminum film.

For the long-wave mode *A*, a distribution characteristic of the surface plasmonic wave [26] is observed — strong binding of the electric field in Si near the boundary with metal in scales much smaller than the wavelength, and exponential attenuation as the distance from this boundary increases (Figure 4). Moreover, the vertical component of the field Ez, oriented perpendicular to the surface as a result of generation of the surface charge in Al [34]. $|E_z|$ component is much higher than $|E_x|$. It is this component that penetrates into QD layer, providing the growth of absorption by means of quantum dots Ge. Mode *A* as a longitudinal-transverse wave is propagating along the direction x, (Figure 5). These circumstances allow us to conclude that the resonance of *A* is excited by a surface plasmon-polariton wave at the boundary of Al-Si.

For modes *B* and *D* the predominant is the field component $|E_x|$ in the heterostructure plane (Figure 4). For *B* peak it is localized in the center of the waveguide layer. For *D* peak the component $|E_x|$ has a node in this area in direction z. Local field maxima are observed near the edge of the hole in Al film, which indicates the formation of hybrid waves representing a superposition of plasmonic and dielectric waveguide modes. The waves *B* and *D* are propagating along the direction y (Figure 5), which allows attributing them to TE_0 and TE_1 hybrid modes of the planar waveguide. It is the generation of these modes that leads to the maximum photocurrent enhancement factor in Figure 3.

The mode *C* also has field components concentrated in the waveguide layer and near the metal boundary. At this wavelength, the vertical component of the electric field has the maximum value. The Poynting vector is directed mainly along y axis, which is typical for the TM waveguide mode. The electric field is concentrated outside the region with quantum dots (Figure 4), and therefore the effect of increased absorption in QDs is small.

4. Conclusion

In conclusion, it should be emphasized that the photoresponse about $2\,\mu$m in heterostructures based on semiconductors group IV was previously observed in GeSn/Ge superlattices [35,36]. The disadvantage of these photodiodes is poor compatibility with modern silicon CMOS technology. In our study, for calibration of the absolute value of spectral sensitivity of photodiodes the structures were irradiated by a series of InGaAsP LED diodes (Roithner Laser Technik) with a set of different wavelengths. Noise characteristics were recorded using SR770 [28] noise analyzer. At the wavelength of $1.98\,\mu$m with reverse bias voltage of 1 V the current sensitivity and detecting capability of a sample with plasmonic grating at room temperature were 1 mA/W and 10^8 cm $\cdot$ Hz$^{1/2}$/W, respectively, which were close to the values (~ 3 mA/W and $\sim 3 \cdot 10^8$ cm $\cdot$ Hz$^{1/2}$/W), obtained in papers [35,36]. Further optimization of the plasmon grating and dielectric waveguide parameters will improve the detection characteristics of silicon heterostructures with quantum dots.

Thus, experimental and theoretical studies were carried out to study the processes of photocurrent and electromagnetic field enhancement in silicon *pin* photodiodes with Ge quantum dots embedded in silicon-on-insulator waveguide structures and integrated with a plasmon grating on the surface of photodiodes. A perforated Al film with a regular arrangement of sub-wavelength holes was used as a plasmon grating. Holes diameter ~ 300 nm, grating period ~ 600 nm. The surface portion occupied by holes in Al, was 19.6%. It was found that maximal enhancement of the photocurrent (up to 8 times) and the intensity of the near field in the wavelength band $\sim 2\,\mu$m is implemented during formation of hybrid waves resulting from the interaction of plasmonic and dielectric waveguide modes.

Acknowledgments

The authors express their thanks for the technological and instrumental support to the Shared Research Facilities

„High Technologies and Nanosystem Analytics“ Novosibirsk State University and „Nanostructures“ of Rzhanov Institute of Semiconductor Physics of the Siberian Branch of the Russian Academy of Sciences.

Funding

The study has been performed under the state assignment of the Ministry of Science and Higher Education of the Russian Federation (topic No. FWGW-2022-0011).

Conflict of interest

The authors declare that they have no conflict of interest.

References

[1] K.L. Wang. Proc. IEEE, **95**, 1866 (2007).
[2] A.V. Dvurechenskii, A.I. Yakimov. In *Advances in semiconductor nanostructures*, ed. by A.V. Latyshev, A.V. Dvurechenskii, A.L. Aseev (Amsterdam, Elsevier, 2017) p. 59.
[3] D. Ahn, C.-Y. Hong, J. Liu, W. Giziewicz, M. Beals, L.C. Kimerling. J. Michel. Opt. Express, **15**, 3916 (2007).
[4] N.J.D. Martinez, C.T. Derose, R.W. Brock, A.L. Starbuck, A.T. Pomerene, A.L. Lentine, D.C. Trotter, P.S. Davids. Opt. Express, **24**, 19072 (2016).
[5] A. Messner, D. Moor, D. Chelladurai, R. Svoboda, J. Smajic, J. Leuthold. APL Photon., **8**, 100901 (2023).
[6] H.R. Stuart, D.G. Hall. Appl. Phys. Lett., **69**, 2327 (1996).
[7] A. Christ, S.G. Tikhodeev, N.A. Gippius, J. Kuhl, H. Giessen. Phys. Rev. Lett., **91**, 183901 (2003).
[8] R.F. Oulton, V.J. Sorger, D.A. Genov, D.F.P. Pile, X. Zhang. Nature Photonics, **2**, 496 (2008).
[9] P.D. Flammer, J.M. Banks, T.E. Furtak, C.G. Durfee, R.E. Hollingsworth, R.T. Collins. Opt. Express, **18**, 21013 (2010).
[10] Y. Bian, Z. Zheng, X. Zhao, L. Liu, Y. Su, J. Liu, J. Zhu, T. Zhou. Phys. Status Solidi A, **210**, 1424 (2013).
[11] M.Z. Alam, J.S. Aitchison, M. Mojahedi. Laser Photon. Rev., **8**, 394 (2014).
[12] F.J. Garcia-Vidal, L. Martin-Moreno, T.W. Ebbesen, L. Kuipers. Rev. Mod. Phys., **82**, 729 (2010).
[13] J. Zhang, L. Zhang, W. Xu. J. Phys. D: Appl. Phys., **45**, 113001 (2012).
[14] N.C. Lindquist, P. Nagpal, K.M. McPeak, D.J. Norris , S.-H. Oh. Rep. Progr. Phys., **75**, 036501 (2012).
[15] W.O.F. Carvalho, J.R. Mejía. Sensors, **20**, 2488 (2020).
[16] S. Hayashi, T. Okamoto. J. Phys. D: Appl. Phys., **45**, 433001 (2012).
[17] C.L. Tan, H. Mohseni. Nanophotonics, **7**, 169 (2018).
[18] C. Peizman, S.-Y. Cho. J. Appl. Phys., **123**, 043107 (2018).
[19] J. Tong, F. Suo, J. Ma, L. Tobing, L. Qian, D. Zhang. Opto-Electron. Adv., **2**, 180026 (2019).
[20] A.I. Yakimov, V.V. Kirienko, A.A. Bloshkin, V.A. Armbrister, A.V. Dvurechenskii. J. Appl. Phys., **122**, 133101 (2017).
[21] A.I. Yakimov, V.V. Kirienko, A.A. Bloshkin, V.A. Armbrister, A.V. Dvurechenskii, J.-M. Hartmann. Opt. Express, **25**, 25602 (2017).
[22] A.I. Yakimov, V.V. Kirienko, V.A. Armbrister, A.A. Bloshkin, A.V. Dvurechenskii. Appl. Phys. Lett., **112**, 171107 (2018).
[23] G. Gu, J. Vaillancourt, P. Vasinajindakaw, X. Lu. Semicond. Sci. Technol., **28**, 105005 (2013).
[24] J. Vaillancourt, N. Mojaverian, X. Lu. IEEE Photon. Technol. Lett., **26**, 745 (2014).
[25] X. Lu, J. Vaillancourt, G. Gu. J. Phys. D: Appl. Phys., **50**, 135101 (2017).
[26] A.I. Yakimov, A.A. Bloshkin, A.V. Dvurechenskii. Photon. Nanostruct., **40**, 100790 (2020).
[27] A.I. Yakimov, V.V. Kirienko, D.E. Utkin, A.V. Dvurechenskii. Nanomaterials, **12**, 2993 (2022).
[28] A.I. Yakimov, V.V. Kirienko, V.A. Armbrister, A.A. Bloshkin, A.V. Dvurechenskii, A.A. Shklyaev. Mater. Res. Express, **3**, 105032 (2016).
[29] H. Zhang, N. Kavanagh, Z. Li, J. Zhao, N. Ye, Y. Chen, N. Wheeler, J.Wooler, J. Hayes, S. Sandoghchi. Opt. Express, **23**, 4946 (2015).
[30] Z. Li, A. Heidt, J. Daniel, Y. Jung, S. Alam, D.J. Richardson. Opt. Express, **21**, 9289 (2013).
[31] D.J. Richardson. Science, **330**, 327 (2010).
[32] V.V. Klimov. *Nanoplazmonika* (M.,Fizmatlit, 2009) (in Russian).
[33] A.D. Rakić, A.B. Djurišić, J.M. Elazar, M.L. Majewski. Appl. Optics, **37**, 5271 (1998).
[34] W.L. Barnes, A. Dereux, T.W. Ebbesen. Nature, **424**, 824 (2003).
[35] T. Pham, W. Du, H. Tran, J. Margetis, J. Tolle, G. Sun, R.A. Soref, H. A. Naseem, B. Li, S.-Qi. Yu. Opt. Express, **24**, 4519 (2016).
[36] H. Zhou, S. Xu, S. Wu, Yi-C. Huang, P. Zhao, J. Tong, B. Son, X. Guo, D. Zhang, X. Gong, C. Seng. Opt. Express, **28**, 34772 (2020).

Translated by T.Zorina